Fat Cell–Specific Ablation of *Rictor* in Mice Impairs Insulin-Regulated Fat Cell and Whole-Body Glucose and Lipid Metabolism

Anil Kumar,[1] John C. Lawrence, Jr.,[1] Dae Young Jung,[2,3] Hwi Jin Ko,[2,3] Susanna R. Keller,[4] Jason K. Kim,[2,3,5] Mark A. Magnuson,[6] and Thurl E. Harris[1]

OBJECTIVE—Rictor is an essential component of mammalian target of rapamycin (mTOR) complex (mTORC) 2, a kinase that phosphorylates and activates Akt, an insulin signaling intermediary that regulates glucose and lipid metabolism in adipose tissue, skeletal muscle, and liver. To determine the physiological role of rictor/mTORC2 in insulin signaling and action in fat cells, we developed fat cell–specific *rictor* knockout (FRic$^{-/-}$) mice.

RESEARCH DESIGN AND METHODS—Insulin signaling and glucose and lipid metabolism were studied in FRic$^{-/-}$ fat cells. In vivo glucose metabolism was evaluated by hyperinsulinemic-euglycemic clamp.

RESULTS—Loss of rictor in fat cells prevents insulin-stimulated phosphorylation of Akt at S473, which, in turn, impairs the phosphorylation of downstream targets such as FoxO3a at T32 and AS160 at T642. However, glycogen synthase kinase-3β phosphorylation at S9 is not affected. The signaling defects in FRic$^{-/-}$ fat cells lead to impaired insulin-stimulated GLUT4 translocation to the plasma membrane and decreased glucose transport. Furthermore, rictor-null fat cells are unable to suppress lipolysis in response to insulin, leading to elevated circulating free fatty acids and glycerol. These metabolic perturbations are likely to account for defects observed at the whole-body level of FRic$^{-/-}$ mice, including glucose intolerance, marked hyperinsulinemia, insulin resistance in skeletal muscle and liver, and hepatic steatosis.

CONCLUSIONS—Rictor/mTORC2 in fat cells plays an important role in whole-body energy homeostasis by mediating signaling necessary for the regulation of glucose and lipid metabolism in fat cells. ***Diabetes*** **59:1397–1406, 2010**

From the [1]Department of Pharmacology, University of Virginia Health System, Charlottesville, Virginia; the [2]Program in Molecular Medicine, University of Massachusetts Medical School, Worcester, Massachusetts; the [3]Department of Medicine, Division of Endocrinology, Metabolism and Diabetes, University of Massachusetts Medical School, Worcester, Massachusetts; the [4]Department of Medicine, Division of Endocrinology, University of Virginia Health System, Charlottesville, Virginia; the [5]Department of Cellular and Molecular Physiology, Pennsylvania State University College of Medicine, Hershey, Pennsylvania; and the [6]Center for Stem Cell Biology and Department of Molecular Physiology and Biophysics, Vanderbilt University Medical Center, Nashville, Tennessee.

Corresponding author: Anil Kumar, al4p@virginia.edu.

Received 19 July 2009 and accepted 8 March 2010. Published ahead of print at http://diabetes.diabetesjournals.org on 23 March 2010. DOI: 10.2337/db09-1061.

Mammalian target of rapamycin (mTOR) is a serine/threonine (S/T) kinase that is a key regulator of cell growth and metabolism (1). mTOR is found in two separate multiprotein complexes: mTOR complex (mTORC) 1, in which mTOR interacts with raptor, mLST8, and PRAS40; and mTORC2, formed by mTOR interaction with rictor, mLST8, and mSin (1–3). mTOR kinase activity associated with mTORC1 can be specifically inhibited by rapamycin (1). When mTOR binds to rictor it is not inhibited by rapamycin (1), but long-term treatment with rapamycin inhibits the formation of mTORC2 in some cell types (4). Both mTORCs are mediators of insulin and growth factor signaling in cultured cells through the classical tyrosine kinase receptor/phosphatidylinositol-3-kinase (PI3K) pathway (1). mTOR complexes phosphorylate and activate a subgroup of the AGC family of protein kinases, including the mTORC1 target S6 kinase 1 (S6K1) (5) and the mTORC2 substrate Akt (also known as protein kinase B) (6). The mTORC1/S6K1 arm of insulin signaling is known to be involved in the regulation of cell growth and protein synthesis (5). Akt mediates insulin regulation of glucose and lipid metabolism in adipose tissue, skeletal muscle, and liver (7).

Full activation of Akt kinase activity requires phosphorylation at S473 by mTORC2 and T308 by phosphoinositide-dependent kinase (PDK1) (8). In cell culture models, short-hairpin RNA (shRNA)-mediated depletion of rictor results in loss of mTORC2-mediated Akt S473 phosphorylation (6). Interestingly, loss of S473 phosphorylation after rictor knockdown in cultured cells reduced the phosphorylation of some, but not all, Akt substrates. The effects of the loss of rictor on insulin-mediated metabolic responses were not tested. Because Akt is downstream of mTORC2 in the insulin signaling pathway and is a mediator of insulin's effect on metabolic processes, we were interested in determining the role of mTORC2 in controlling glucose and lipid metabolism in insulin target tissues. Since whole-body *rictor* knockout mice are embryonic lethal (9,10), we previously developed mice in which *rictor* expression was ablated specifically in skeletal muscle (MRic$^{-/-}$) (11). MRic$^{-/-}$ mice exhibited impaired insulin-stimulated Akt S473 phosphorylation and glucose transport defects in skeletal muscles that resulted in mild glucose intolerance.

Recently, adipose tissue has gained increased attention not only for storing body's excess energy but also as an endocrine organ secreting adipokines, such as leptin, adiponectin, and resistin (12). The adipokines, as well as nonesterified fatty acids (NEFAs) formed during lipolysis in fat cells, impact whole-body insulin sensitivity and insulin secretion by pancreatic β-cells (13). mTOR has

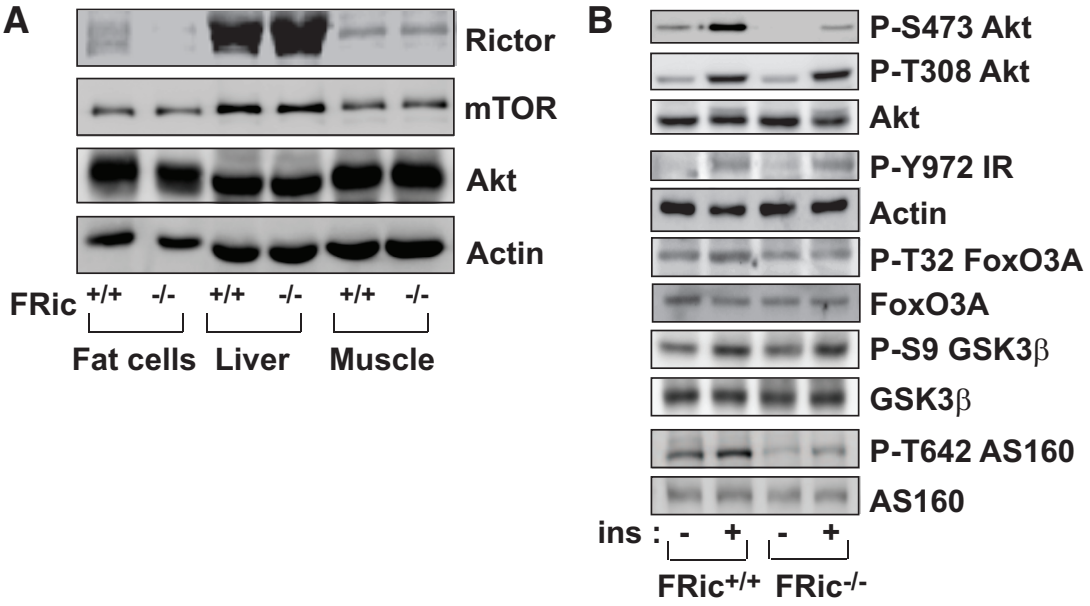

FIG. 1. Analysis of rictor expression and insulin signaling in FRic$^{-/-}$ fat cells. *A*: Lack of rictor protein in FRic$^{-/-}$ fat cells. Tissue extracts prepared from isolated fat cells, liver, and skeletal muscle were subjected to SDS-PAGE (6.5% gel) and immunoblotted with anti-rictor antibody (*top*). The immunoblots for mTOR, Akt, and actin (loading control) are shown in the bottom panels. *B*: Insulin signaling in isolated FRic$^{-/-}$ fat cells. Immunoblot analysis of insulin (ins)-stimulated phosphorylation of Akt at S473, Akt at T308, IR at Y972, FoxO3A at T32, GSK-3β at S9, and AS160 at T642 in FRic$^{-/-}$ and FRic$^{+/+}$ fat cells (shown here are representative immunoblots, four mice for each genotype were analyzed). Also shown are immunoblots of total Akt, FoxO3A, GSK-3β, and AS160 used for normalizing the corresponding anti-phospho immunoblots.

been implicated in fat cell function (1). Patients treated with rapamycin have elevated circulating NEFAs, suggesting that mTORC1 plays a role in the regulation of fat cell lipolysis (14,15). However, because chronic rapamycin treatment can affect the activity of both mTORC1 and mTORC2 (4), it was unclear which complex was involved in the regulation of lipolysis in adipocytes. As demonstrated in fat cell–specific *GLUT4* (insulin-responsive GLUT) knockout mice (16), glucose transport by fat cells is critical for the maintenance of whole-body glucose homeostasis. Our study with MRic$^{-/-}$ mice had shown a role for rictor/mTORC2 in the regulation of glucose uptake (11). To determine the role of rictor/mTORC2 in fat cell function and the regulation of glucose and lipid metabolism, we developed mice in which *rictor* expression was specifically ablated in fat cells (FRic$^{-/-}$ mice).

RESEARCH DESIGN AND METHODS

Generation of FRic$^{-/-}$ mice. *Rictor*$^{flox/flox}$ mice (10) were crossed with *aP2-cre* transgenic mice [strain, B6-Cg-Tg(Fabp4-cre)1Rev/J; The Jackson Laboratory, Bar Harbor, ME] to obtain heterozygous *aP2-cre;rictor*$^{flox/WT}$ offspring (where WT refers to wild type) in the F1 generation. These heterozygous mice were crossed with *rictor*$^{flox/flox}$ mice to obtain the FRic$^{-/-}$ mice with genotype *aP2-cre;rictor*$^{flox/flox}$ and their *rictor*$^{flox/flox}$ littermates lacking aP2-Cre expression (referred to here as FRic$^{+/+}$). Age-matched FRic$^{+/+}$ and FRic$^{-/-}$ mice of both sexes were studied at 3–5 months of age (young) and when they were aged >9 months (old). For all mice used, the genotypes were determined by PCR analysis of tail genomic DNA as described previously (10). Both *rictor*$^{flox/flox}$ mice as well as *aP2-cre* transgenic mice used for breeding had been backcrossed for 6 and 9 generations to the C57BL/6 strain, respectively. The mice were maintained under temperature- and humidity-controlled conditions with a 12-h light/dark cycle and were allowed food (total calories from fat 17%, LM-485; Harlan-Teklad) and water ad libitum. All animal studies performed in this investigation were approved by the University of Virginia Animal Care and Use Committee.

Hyperinsulinemic-euglycemic clamps. Following an overnight fast (~15 h), a 2-h hyperinsulinemic (insulin at 150 mU/kg body wt priming followed by 2.5 mU/kg/min)-euglycemic clamp was conducted in awake mice using [3-^{3}H]-glucose and 2-deoxy-D-[1-^{14}C]-glucose to assess glucose metabolism in individual tissues as described in Kim et al. (17). Other experimental protocols are described in detail in the online appendix (available at http://diabetes.diabetesjournals.org/cgi/content/full/dc09-1061/DC1).

Statistics. Values given are means ± SE for the numbers of animals indicated in the figure legends. Significance was determined by unpaired two-tailed *t* tests. Differences were considered significant if the *P* value was <0.05.

RESULTS

Ablation of *rictor* in fat cells impairs insulin signaling. FRic$^{-/-}$ mice were generated by breeding *rictor*$^{flox/flox}$ mice with mice expressing Cre recombinase under the control of the *aP2* promoter. Rictor protein levels were measured in isolated fat cells, liver, and skeletal muscle from FRic$^{-/-}$ and FRic$^{+/+}$ littermates. While fat cells from FRic$^{-/-}$ mice showed an ~90% reduction ($P < 0.0001$) in rictor protein levels when compared with FRic$^{+/+}$ fat cells, there was no change in rictor protein levels in liver and skeletal muscle of FRic$^{-/-}$ mice (Fig. 1*A*). This result confirmed that the aP2-Cre–mediated recombination event was restricted to fat cells. mTOR, the binding partner of rictor in mTORC2, and Akt, a known substrate of mTORC2 kinase, were expressed at similar levels in FRic$^{-/-}$ and FRic$^{+/+}$ fat cells (Fig. 1*A*).

To test the effect of loss of rictor on mTORC2 activity, we measured levels of Akt phosphorylation at the S473 residue in insulin-stimulated FRic$^{+/+}$ and FRic$^{-/-}$ fat cells. Consistent with the data we obtained in MRic$^{-/-}$ muscles (11), in FRic$^{-/-}$ fat cells insulin caused only a threefold increase in Akt phosphorylation at S473, whereas in FRic$^{+/+}$ fat cells an ~10-fold increase above the basal level was observed (Fig. 1*B*). This result suggests that mTORC2 is the major kinase responsible for phosphorylating Akt at the S473 residue in response to insulin in fat cells.

Similar to what we had previously reported in MRic$^{-/-}$ mice (11), the level of Akt phosphorylation at T308 (a site phosphorylated by PDK1) in insulin-stimulated FRic$^{-/-}$ fat cells was comparable with that seen in FRic$^{+/+}$ fat cells

(Fig. 1*B*). Also, insulin-stimulated phosphorylation of the insulin receptor (IR) at the tyrosine (Y) 972 residue was normal (Fig. 1*B*). When evaluating phosphorylation of Akt substrates in response to insulin, we found that in FRic$^{-/-}$ and FRic$^{+/+}$ fat cells phosphorylation of glycogen synthase kinase (GSK) 3β at S9 was similar between the two genotypes (Fig. 1*B*). However, phosphorylation of both FoxO3a at T32 (Fig. 1*B*) and AS160 at T642 was dramatically reduced (69% reduction in insulin-stimulated AS160 T642 phosphorylation in FRic$^{-/-}$ fat cells, $P < 0.03$) (Fig. 1*B*). FoxO3a is also shown to be phosphorylated at T32 by serum- and glucocorticoid-induced protein kinase (SGK) 1, another target of mTORC2 kinase activity (18). However, in insulin-stimulated fat cells, whether mTORC2 mediates SGK1 phosphorylation is not known. Recently, mTORC2 has been reported to promote the phosphorylation of turn motif sites in protein kinase C (PKC) α, thus mediating its stabilization (19,20). In mTORC2-null FRic$^{-/-}$ fat cells, we observed a decrease in PKCα levels ($P < 0.001$; supplemental Fig. 1).

Loss of *rictor* does not affect fat mass and fat cell size but increases organ weights. Body composition of FRic$^{-/-}$ and FRic$^{+/+}$ mice, assessed by proton–magnetic resonance spectroscopy, showed similar fat and lean mass (supplemental Fig. 2*A*). Also, fat cell sizes of FRic$^{-/-}$ and FRic$^{+/+}$ mice were not different (supplemental Fig. 2*B* and *C*). However, as previously reported (21), parametrial fat pads (40%), pancreas (20%), kidney (24%), liver (19%), and heart (22%) were heavier in FRic$^{-/-}$ mice compared with FRic$^{+/+}$ mice (supplemental Fig. 3).

Loss of *rictor* impairs glucose transport in fat cells. Consistent with previous findings demonstrating decreased glucose transport in skeletal muscle lacking rictor (11), glucose transport was reduced in FRic$^{-/-}$ fat cells. While insulin caused a three- to fourfold increase ($P < 0.004$) in glucose uptake above basal levels in both FRic$^{+/+}$ and FRic$^{-/-}$ fat cells (Fig. 2*A*), in FRic$^{-/-}$ fat cells basal as well as insulin-stimulated glucose uptake were reduced by ~75% ($P < 0.0002$) and ~65% ($P < 0.002$), respectively, when compared with FRic$^{+/+}$ fat cells.

To elucidate the possible defect underlying the reduction in glucose uptake in FRic$^{-/-}$ fat cells, we analyzed the expression of proteins known to be essential for insulin-stimulated glucose uptake. Total levels of the GLUT4 (Fig. 2*B*), the insulin-regulated aminopeptidase (IRAP), a protein associated with GLUT4 (22), and myosin 1c (Myo1c), a protein involved in insulin-regulated GLUT4 translocation to the plasma membrane (23), were similar in FRic$^{-/-}$ and FRic$^{+/+}$ fat cells (Fig. 2*B*). However, the amount of GLUT4 in plasma membranes prepared from basal and insulin-stimulated FRic$^{-/-}$ fat pads was reduced by ~40% when compared with plasma membranes prepared from FRic$^{+/+}$ fat pads ($n = 3$, $P < 0.01$ for basal and $P < 0.05$ for insulin stimulated) (Fig. 2*C*, *upper and lower panels*, and *D*).

Dysregulation of lipolysis in FRic$^{-/-}$ mice. When measuring serum metabolite levels, we found normal fed and slightly decreased fasting triglyceride (TAG) levels ($P < 0.04$) (Table 1) in FRic$^{-/-}$ mice (Table 1). Glycerol levels in serum from fasted ($P < 0.01$) (Table 1) and fed ($P < 0.02$) (Table 1) male FRic$^{-/-}$ mice were higher compared with FRic$^{+/+}$ mice. Similarly, female FRic$^{-/-}$ mice had elevated glycerol levels (3- to 5-month-old fed mice, 12.9 ± 2.4 μg/ml in FRic$^{+/+}$ mice and 24.5 ± 4.3 μg/ml in FRic$^{-/-}$ mice, $n = 5–6$, $P = 0.057$). In addition, fasting NEFA levels were increased significantly ($P < 0.04$) (Table 1) in FRic$^{-/-}$ mice, while fed NEFA levels were unchanged (Table 1).

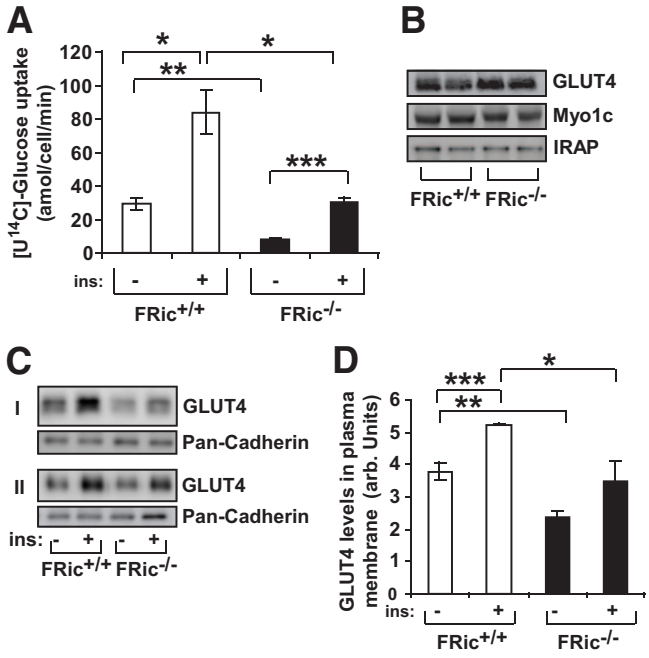

FIG. 2. Glucose uptake in FRic$^{-/-}$ fat cells. *A*: [U^{14}C]-glucose uptake in fat cells isolated from FRic$^{+/+}$ and FRic$^{-/-}$ mice (3- to 5-month-old female mice, $n = 4$, *$P < 0.004$; **$P < 0.0002$; ***$P < 0.0001$). *B*: Representative immunoblots of isolated FRic$^{-/-}$ and FRic$^{+/+}$ fat cell extracts from 3- to 5-month-old female mice, probed for GLUT4, Myo1c, and IRAP ($n = 5$). *C*: Immunoblots showing GLUT4 levels in plasma membrane isolated from basal and insulin-stimulated fat pads from FRic$^{-/-}$ and FRic$^{+/+}$ mice (3- to 5-month-old female, representative blots of two sets of FRic$^{+/+}$ and FRic$^{-/-}$ fat pads labeled as I and II out of a total of three sets). Cadherin levels in plasma membrane determined by immunoblotting with pan-cadherin antibody served as the loading control for plasma membrane preparations (*middle panel*). *D*: The GLUT4 quantification data (means ± SE) shows band intensity of GLUT4 after normalization to the levels of cadherin detected in the same sample ($n = 3$, *$P < 0.05$; **$P < 0.01$ and ***$P < 0.006$). arb., arbitrary. ins, insulin.

Since serum levels of both NEFAs and glycerol, the products of lipolysis, were elevated in FRic$^{-/-}$ mice (Table 1), we examined whether FRic$^{-/-}$ mice are resistant to insulin-induced inhibition of lipolysis. To test this

TABLE 1
Serum insulin, metabolite, and adipokine levels in FRic$^{-/-}$ mice

	FRic$^{+/+}$	FRic$^{-/-}$
Triglycerides (mg/dl)		
Fasting	41.4 ± 1.6	35.7 ± 1.9*
Fed	53.1 ± 1.5	49.8 ± 3.8
Glycerol (μg/ml)		
Fasting	19.7 ± 2.9	30.5 ± 2.5*
Fed	23.7 ± 2.8	34.8 ± 3.4*
NEFAs (mEq/l)		
Fasting	0.75 ± 0.05	1.01 ± 0.04*
Fed	0.82 ± 0.04	0.88 ± 0.04
Insulin (ng/ml)		
Fasting	0.15 ± 0.02	0.45 ± 0.09*
Fed	0.39 ± 0.06	3.4 ± 0.6*
Adiponectin (μg/ml)	14.1 ± 1.7	16.2 ± 1.7
Leptin (ng/ml)	7.7 ± 1.3	8.0 ± 1.6
Resistin (ng/ml)	15.6 ± 0.7	15.3 ± 1.5

Data are means ± SE. Male mice, aged 3–5 months, $n = 5–9$. *$P < 0.05$ vs. FRic$^{+/+}$ mice of the same group.

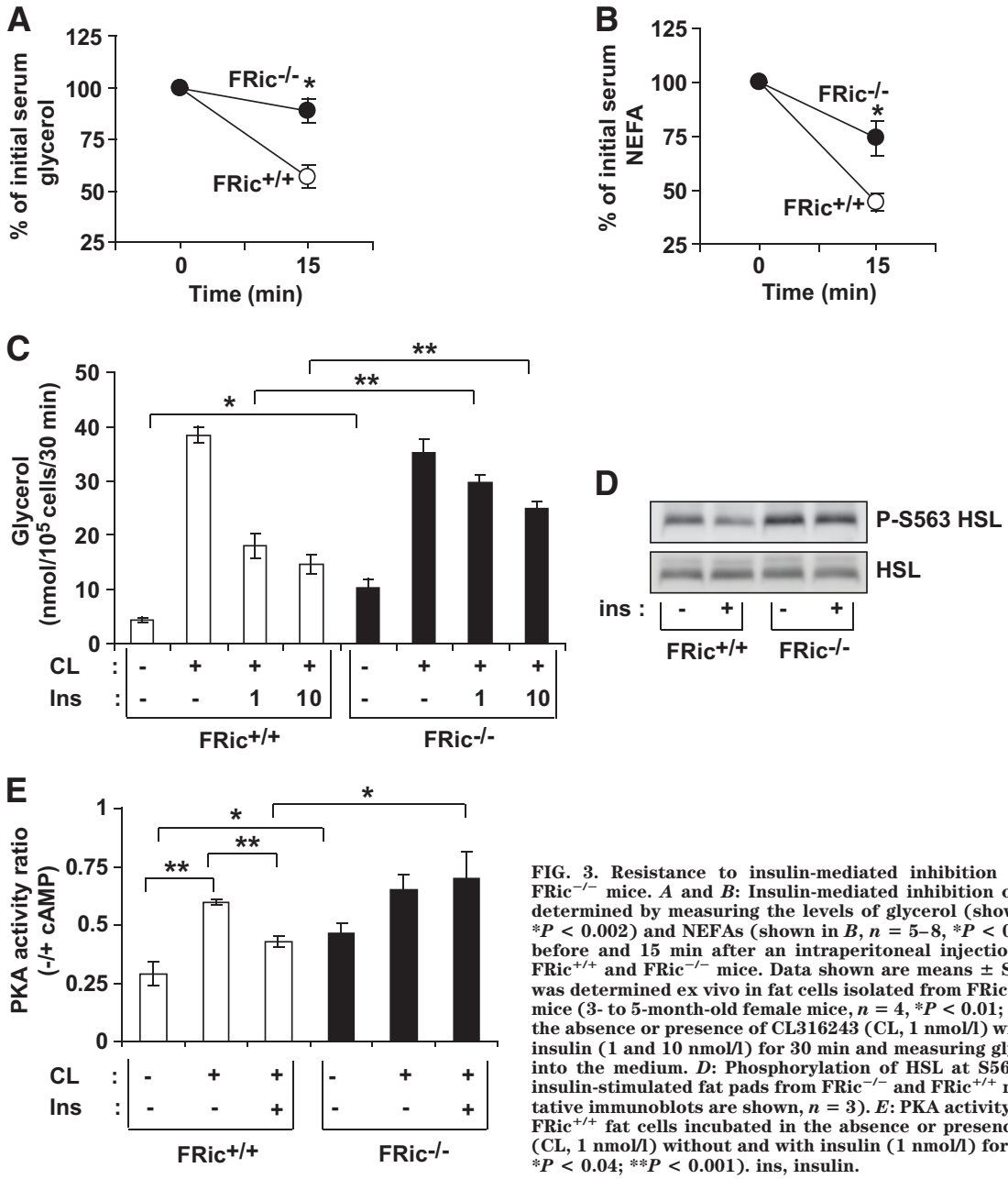

FIG. 3. Resistance to insulin-mediated inhibition of lipolysis in FRic$^{-/-}$ mice. *A* and *B*: Insulin-mediated inhibition of lipolysis was determined by measuring the levels of glycerol (shown in *A*, $n = 8$, $^*P < 0.002$) and NEFAs (shown in *B*, $n = 5$–8, $^*P < 0.004$) in serum before and 15 min after an intraperitoneal injection of insulin in FRic$^{+/+}$ and FRic$^{-/-}$ mice. Data shown are means ± SE. *C*: Lipolysis was determined ex vivo in fat cells isolated from FRic$^{-/-}$ and FRic$^{+/+}$ mice (3- to 5-month-old female mice, $n = 4$, $^*P < 0.01$; $^{**}P < 0.001$) in the absence or presence of CL316243 (CL, 1 nmol/l) without and with insulin (1 and 10 nmol/l) for 30 min and measuring glycerol released into the medium. *D*: Phosphorylation of HSL at S563 in basal and insulin-stimulated fat pads from FRic$^{-/-}$ and FRic$^{+/+}$ mice (representative immunoblots are shown, $n = 3$). *E*: PKA activity in FRic$^{-/-}$ and FRic$^{+/+}$ fat cells incubated in the absence or presence of CL316243 (CL, 1 nmol/l) without and with insulin (1 nmol/l) for 10 min ($n = 4$, $^*P < 0.04$; $^{**}P < 0.001$). ins, insulin.

in vivo, we determined the levels of glycerol and NEFAs in serum taken from FRic$^{-/-}$ and FRic$^{+/+}$ mice before and 15 min after an intraperitoneal insulin injection (16). In FRic$^{+/+}$ mice, insulin caused an ~50% reduction in both glycerol and NEFA levels, indicating inhibition of lipolysis by insulin (Fig. 3*A*), whereas in FRic$^{-/-}$ mice there was only a 13% reduction in glycerol levels ($n = 8$, $P < 0.002$ vs. FRic$^{+/+}$ mice) (Fig. 3*A*). Serum NEFA levels also declined significantly less after insulin injection in FRic$^{-/-}$ mice compared with FRic$^{+/+}$ mice ($n = 5$–8, $P < 0.004$) (Fig. 3*B*). We next evaluated lipolysis ex vivo by determining glycerol release from isolated FRic$^{-/-}$ and FRic$^{+/+}$ fat cells in the presence of either CL316243 (specific β3-adrenergic receptor agonist) alone to induce lipolysis and CL316243 together with insulin to suppress lipolysis. As shown in Fig. 3*C*, FRic$^{-/-}$ fat cells showed twofold higher levels of basal lipolysis ($n = 4$, $P < 0.01$) when compared with FRic$^{+/+}$ fat cells, but the levels of CL316243-stimulated lipolysis was similar between FRic$^{-/-}$ and FRic$^{+/+}$ fat cells (Fig. 3*C*). Insulin suppressed CL316243-induced lipolysis in FRic$^{+/+}$ fat cells by ~50% ($n = 4$, $P < 0.0001$) (Fig. 3*C*) but in FRic$^{-/-}$ fat cells only by 15% ($n = 4$) (Fig. 3*C*). These data clearly demonstrate a defective regulation of lipolysis in FRic$^{-/-}$ mice.

Insulin suppresses lipolysis largely through the regulation of hormone-sensitive lipase (HSL). Phosphorylation of HSL at S563 by cAMP-dependent protein kinase (also known as protein kinase A, PKA) increases the lipolytic activity of HSL, and insulin suppresses HSL activity by inhibiting the activation of PKA (24,25). Although HSL levels were similar in isolated fat pads of both genotypes (Fig. 3*D*), there was an increased basal level of phosphorylation of HSL at S563 in FRic$^{-/-}$ compared with FRic$^{+/+}$ fat pads (Fig. 3*D*). Furthermore, whereas an ~30% reduction in HSL S563 phosphorylation was observed in FRic$^{+/+}$ fat pads, no repression of HSL S563 phosphorylation was found in FRic$^{-/-}$ fat pads in response to insulin ($n = 3$) (Fig. 3*D*). Isoproterenol (a β-adrenergic receptor agonist)

and CL316243 are known to stimulate HSL S563 phosphorylation by inducing cAMP production and consequently activating PKA. In isolated fat pads, isoproterenol stimulated HSL S563 phosphorylation in both FRic$^{-/-}$ and FRic$^{+/+}$ fat pads (supplemental Fig. 4). However, the insulin-mediated inhibition of isoproterenol-induced HSL S563 phosphorylation was seen only in FRic$^{+/+}$ fat pads (supplemental Fig. 4). Consistent with these findings, basal PKA activity in isolated FRic$^{-/-}$ fat cells was 50% higher ($n = 4$, $P < 0.01$) (Fig. 3*E*) than in FRic$^{+/+}$ fat cells, but CL316243 stimulated PKA activity in FRic$^{-/-}$ and FRic$^{+/+}$ fat cells to a similar level. Insulin suppressed CL316243-mediated activation of PKA in FRic$^{+/+}$ fat cells by 50% ($n = 4$, $P < 0.001$) (Fig. 3*E*) but had no effect in FRic$^{-/-}$ fat cells ($n = 4$) (Fig. 3*E*). This finding, together with reduced repression of lipolysis in insulin-stimulated FRic$^{-/-}$ fat cells, strongly supports a role for rictor/mTORC2 in the regulation of PKA activity to suppress lipolysis in fat cells.

Rictor/mTORC2 in fat cells regulates whole-body glucose homeostasis. Fat cell function affects whole-body glucose homeostasis and insulin sensitivity (26). In FRic$^{-/-}$ mice, serum insulin levels were significantly higher than in FRic$^{+/+}$ mice (for fasting, $P < 0.008$; for fed, $P < 0.0001$) (Table 1). Furthermore, young FRic$^{-/-}$ mice showed impaired insulin sensitivity in insulin tolerance tests (supplemental Fig. 5*C*). Younger FRic$^{-/-}$ mice (3–5 months old) of either sex showed slightly better glucose clearance during a glucose tolerance test when compared with FRic$^{+/+}$ controls (supplemental Fig. 5*A*) as previously reported (21). However, old FRic$^{-/-}$ mice (>9 months old) showed significantly higher blood glucose levels after an overnight fast and a dramatic impairment in glucose clearance after an intraperitoneal glucose load (Fig. 4*A* and supplemental Fig. 5*B*). These data indicate the presence of severe insulin resistance in young and old FRic$^{-/-}$ mice.

To measure insulin sensitivity in individual tissues, we performed a 2-h hyperinsulinemic-euglycemic clamp in conscious young male FRic$^{-/-}$ mice. During the clamp, the glucose infusion rate required to maintain euglycemia (Fig. 4*B*), and insulin-stimulated whole-body glucose turnover rates (Fig. 4*C*) were significantly lower in the FRic$^{-/-}$ mice compared with FRic$^{+/+}$ mice (glucose infusion rate, 80% reduction $P < 0.0001$; glucose turnover rate, 49% reduction, $P < 0.0001$), indicating pronounced systemic insulin resistance in FRic$^{-/-}$ mice. Insulin-stimulated whole-body glycolysis (Fig. 4*D*) and glycogen plus lipid synthesis (Fig. 4*E*) were also reduced in FRic$^{-/-}$ mice when compared with FRic$^{+/+}$ mice (glycolysis, ~44% reduction, $P < 0.01$; glycogen plus lipid synthesis, ~59% reduction, $P < 0.001$). As shown in Fig. 4*F* and *G*, in vivo insulin-stimulated glucose uptake in adipose tissue and skeletal muscle during the hyperinsulinemic-euglycemic clamp was also significantly reduced in FRic$^{-/-}$ mice (~50% reduction in adipose tissue, $P < 0.01$; ~33% reduction in skeletal muscle, $P < 0.04$). In addition, insulin induced a marked suppression of hepatic glucose production (HGP) during the clamp in FRic$^{+/+}$ mice (46% reduction compared with basal levels, $P < 0.001$) (Fig. 4*H*); however, insulin completely failed to suppress HGP in FRic$^{-/-}$ mice (Fig. 4*H*). These results point not only to severe insulin resistance in adipose tissue but also marked insulin resistance in skeletal muscle and liver of FRic$^{-/-}$ mice.

Adipokines can affect whole-body insulin sensitivity. However, we found that serum levels of leptin, adiponectin, and resistin were similar in FRic$^{-/-}$ and FRic$^{+/+}$ mice (Table 1). This result shows that changes in at least these adipokines do not play a causative role in the reduced insulin sensitivity in FRic$^{-/-}$ mice.

Decreased glucose metabolism, impaired insulin signaling, and increased lipid accumulation in skeletal muscles of FRic$^{-/-}$ mice. Since fat cell–specific loss of rictor/mTORC2 decreased skeletal muscle glucose transport in response to insulin, we measured insulin-stimulated glycogen synthesis in isolated soleus and extensor digitorum longus (EDL) muscles. We found that insulin-stimulated glycogen synthesis was markedly reduced in both soleus (~41% reduction, $P < 0.0001$) (Fig. 5*A*) and EDL (~27% reduction, $P < 0.0004$) (supplemental Fig. 6) muscles from FRic$^{-/-}$ mice when compared with FRic$^{+/+}$ mice. The isolated EDL muscle from FRic$^{-/-}$ mice showed normal insulin-stimulated phosphorylation of the IR at Y972. However, a marked reduction in insulin-stimulated phosphorylations of insulin receptor substrate (IRS) 1 at Y896 and of Akt at both T308 and S473 (Fig. 5*B*) was observed. Interestingly, basal phosphorylation of IRS1 at S302 in isolated EDL muscles from FRic$^{-/-}$ mice was slightly increased when compared with FRic$^{+/+}$ mice (~30%, $n = 4$, data not shown). In addition, we found a twofold increase ($P < 0.03$) in levels of IRS1 phosphorylated at S302 (Fig. 5*C*, *top panel*) and a 37% reduction ($P < 0.04$) in the total IRS1 (Fig. 5*C*, *middle panel*) levels in tibialis anterior (TA) muscles from FRic$^{-/-}$ mice.

Since the FRic$^{-/-}$ mice showed increased lipolysis and muscle is known to take up NEFAs to store as TAG, we measured TAG levels in TA muscle homogenates. Indeed TAG levels in muscles from FRic$^{-/-}$ mice were significantly increased when compared with FRic$^{+/+}$ mice ($P < 0.04$) (Fig. 5*D*). Consistent with the increase in TAG levels, we found that lipin 1, an enzyme involved in the synthesis of TAG (27), was increased (1.4-fold, $P < 0.002$) in the TA muscles of FRic$^{-/-}$ mice (Fig. 5*E*, *top panel*). Thus, the loss of rictor in fat cells leads to increased lipid deposition and impaired insulin signaling in skeletal muscle.

FRic$^{-/-}$ mice develop hepatic steatosis. Livers from both young and old FRic$^{-/-}$ mice showed increased lipid accumulation (hepatic steatosis) when compared with age-matched FRic$^{+/+}$mice (Fig. 6*A* and *B*). Consistent with this finding, gene expression of two important hepatic lipogenic enzymes, L-type pyruvate kinase (L-PK) and fatty acid synthase (FAS) were increased two- and threefold, respectively, in livers from old FRic$^{-/-}$ mice ($P < 0.05$) (Fig. 6*C* and *D*).

DISCUSSION

The loss of fat cell *rictor* expression in mice results in a metabolic phenotype similar to type 2 diabetes with impaired fat cell function associated with severe insulin resistance in adipose tissue, skeletal muscle, and liver. This suggests that rictor plays an important role in regulating fat cell metabolism and, consequently, whole-body glucose and lipid homeostasis and insulin sensitivity.

FRic$^{-/-}$ fat cells showed impaired regulation of glucose transport and lipolysis in response to insulin. Defective insulin signaling in FRic$^{-/-}$ fat cells most likely causes these metabolic abnormalities. Our analyses of insulin signaling events that lie downstream of mTORC2 and mediate metabolic responses revealed a dramatic reduction in phosphorylation of Akt at S473 and, consequently,

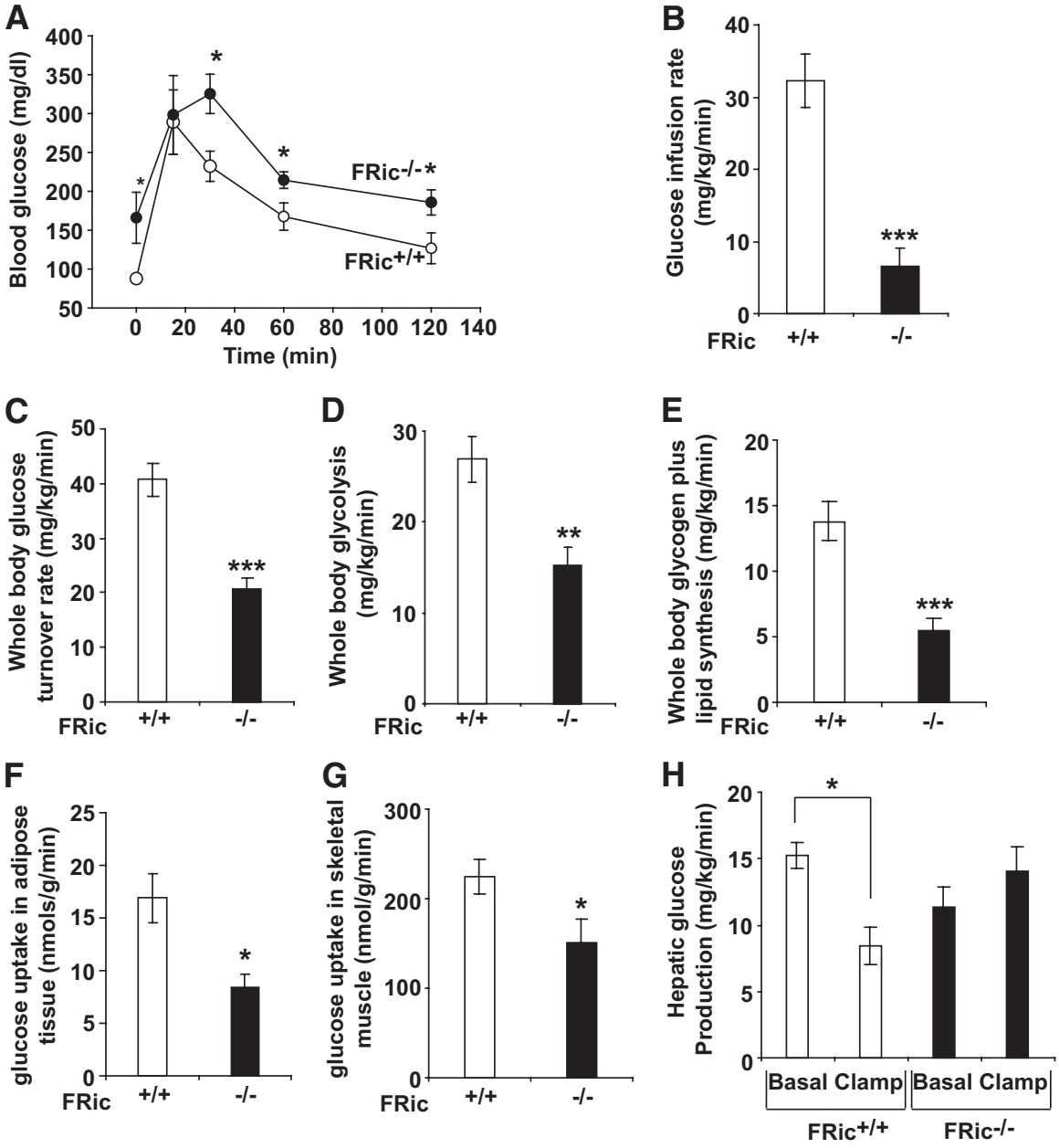

FIG. 4. Glucose homeostasis in male FRic$^{-/-}$ mice. *A*: Intraperitoneal glucose tolerance tests in old male FRic$^{-/-}$ and FRic$^{+/+}$ mice (>9 months old, $n = 4$, *$P < 0.05$). *B–F*: Whole-body glucose homeostasis in young FRic$^{-/-}$ and FRic$^{+/+}$ mice as evaluated by hyperinsulinemic-euglycemic clamp. *B*: Glucose infusion rate. *C*: Glucose turnover rate. *D*: Glycolysis. *E*: Glycogen plus lipid synthesis. *F*: Glucose uptake in adipose tissue. *G*: glucose uptake in skeletal muscle. *H*: hepatic glucose production (3- to 4-month-old male mice, $n = 5–6$ per group. *B–H*: *$P < 0.04$; **$P < 0.001$; ***$P < 0.0001$). Data shown are means ± SE.

FoxO3a at T32 and AS160 at T642. At this time, it is not clear whether FoxO3a has a role in the observed metabolic defects in FRic$^{-/-}$ fat cells. However, the Akt-mediated AS160 phosphorylation at T642 and consequent inhibition of the Rab-GAP (GTPase activating protein) activity of AS160 is essential for insulin-stimulated GLUT4 translocation to the plasma membrane (28,29). Consistent with decreased phosphorylation of AS160, GLUT4 translocation to the plasma membrane in response to insulin is impaired and glucose uptake is decreased in FRic$^{-/-}$ fat cells.

Rictor/mTORC2 activity has not been linked to regulation of either basal lipolysis or insulin-mediated suppression of lipolysis. However, our observations that in FRic$^{-/-}$ fat cells increased phosphorylation of HSL at S563 concomitant with upregulated PKA activity and that insulin failed to inhibit these events suggests a role for mTORC2 in the regulation of lipolysis by modifying PKA and HSL activities. It is not clear how mTORC2 regulates basal PKA activity. In response to insulin, Akt directly phosphorylates and activates phosphodiesterase 3B (PDE3B) (30) increasing cAMP to AMP conversion and thereby decreasing PKA activity (31). Since PKA activates lipolysis via phosphorylation of HSL, a defect in insulin activation of PDE3B would impair downregulation of lipolysis. In fact, defective regulation of lipolysis in response to insulin is reported in PDE3B knockout mice (32). While our data supports a model whereby mTORC2 activity controls Akt-mediated activation of PDE3B by insulin, this remains to be established. Rapamycin-mediated inhibition of mTOR has implicated mTORC1 in the

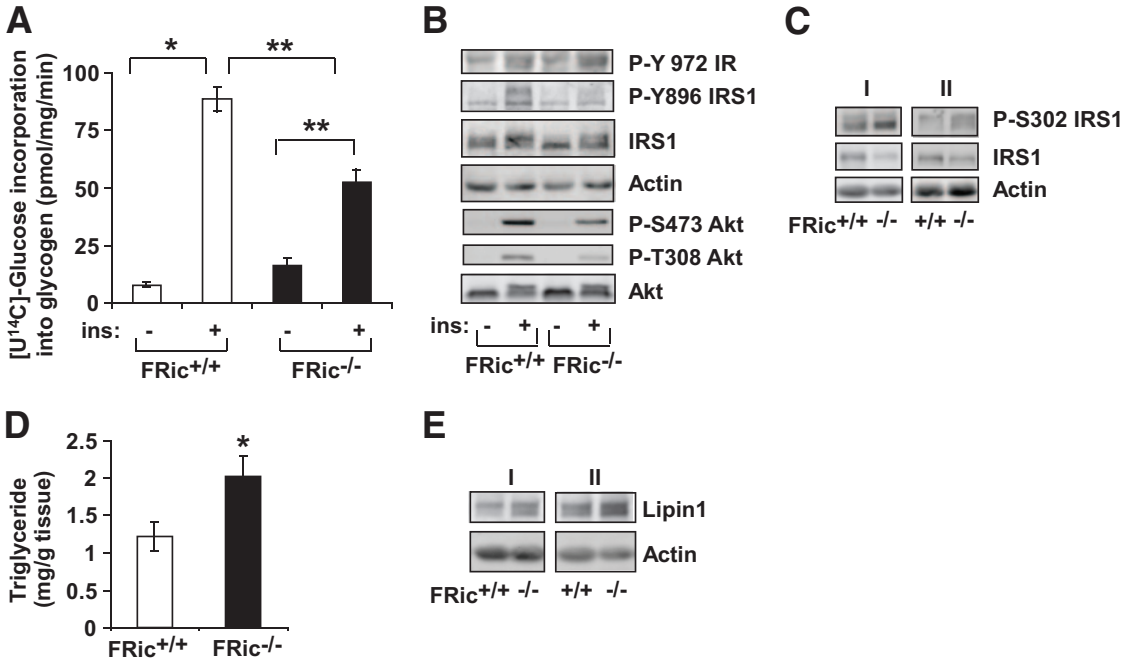

FIG. 5. Glucose and lipid metabolism and insulin signaling in skeletal muscles from FRic$^{-/-}$ mice. *A*: Insulin-stimulated glycogen synthesis in ex vivo–incubated soleus muscles (female, 3–5 months old, $n = 4–5$, *$P < 0.02$; **$P < 0.0001$) from FRic$^{-/-}$mice using [U^{14}C]-glucose. *B*: Insulin signaling in isolated EDL muscles from FRic$^{+/+}$ and FRic$^{-/-}$ mice. Protein extracts prepared from EDL muscles stimulated without or with 20 mU of insulin for 30 min were immunoblotted with phospho-specific antibodies to the Y-972 residue of IR, the Y896 residue of IRS1, and the T308 and S473 residues of Akt (representative blot is shown, $n = 3–4$). *C*: In vivo total and phosphorylated IRS1 at S302. Protein extracts prepared from TA muscles of fed FRic$^{+/+}$ and FRic$^{-/-}$ mice were immunoblotted using antibodies against phospho-S302 IRS1 (P-S302 IRS1), total IRS1, and actin (female, 3–5 months old, representative blots of two sets of FRic$^{+/+}$ and FRic$^{-/-}$ mice labeled as I and II out of a total of eight sets). *D*: Triglyceride levels in skeletal muscle homogenates prepared from fed FRic$^{+/+}$ and FRic$^{-/-}$ mice (3- to 5-month-old female, $n = 5–6$, *$P < 0.04$). Data shown are means ± SE. *E*: Protein extracts prepared from TA muscles of fed FRic$^{+/+}$ and FRic$^{-/-}$ mice were immunoblotted for lipin1 and actin (3- to 5-month-old female mice, representative blots of two sets of FRic$^{+/+}$ and FRic$^{-/-}$ mice labeled as I and II out of a total of eight sets). ins, insulin.

regulation of lipolysis (14,15); however, eliminating mTORC1 by ablating *raptor* in fat cells does not affect lipolysis (33). Considering that prolonged rapamycin treatment inhibits the formation of mTORC2 in some cell types (4), our studies suggest that clinical observations of elevated NEFA levels during rapamycin treatment (14,15) could be due to inhibition of mTORC2.

How do fat cell–specific genetic alterations in the insulin signaling pathway lead to impairment of whole-body glucose homeostasis? Although FRic$^{-/-}$ mice show a profound reduction in glucose transport in fat cells, this defect is likely to be only partly responsible for impaired glucose homeostasis in the FRic$^{-/-}$ mice. Adipose tissue contributes only ~10% to whole-body glucose clearance (34). The major contributors to impaired glucose homeostasis in FRic$^{-/-}$ mice are reduced insulin-stimulated skeletal muscle glucose transport and impaired suppression of hepatic glucose production by insulin. We propose that elevated circulating NEFAs due to upregulation of lipolysis in fat cells cause the insulin resistance in skeletal muscle and liver observed in the FRic$^{-/-}$ mice.

The increased serum NEFA levels in FRic$^{-/-}$ mice are most likely responsible for the elevated intramuscular accumulation of TAG, which in turn may be mediated by increased lipin 1 levels in FRic$^{-/-}$ skeletal muscles. Increased NEFAs flux into skeletal muscle leads to elevated intramuscular levels of lipid metabolites, such as fatty acyl CoA and diacylglycerol (35). These lipids induce insulin resistance in skeletal muscle by causing defects in insulin signaling (36). Previously, NEFAs have been shown to activate serine/threonine kinases such as IκB kinase-2 (37), Jun NH_2-terminal kinase (38), and protein kinase Cθ (39). All of these kinases can phosphorylate IRS1 on critical serine residues, thereby blocking phosphorylation of IRS1 by IR kinase on tyrosine sites that are required for PI3K association and activation (40). IRS1 S302 phosphorylation through IκB kinase-2 (41) or Jun NH_2-terminal kinase (42) can lead to IRS1 degradation. Since we see an increase in phosphorylation of IRS1 at S302 in FRic$^{-/-}$ muscle, a decrease in IRS1 Y896 phosphorylation, as well as a reduction in total IRS1 levels, we suggest that elevated lipids are responsible for the insulin resistance observed in vivo and ex vivo in the skeletal muscles of FRic$^{-/-}$ mice.

The development of hepatic steatosis in FRic$^{-/-}$ mice may be due to the prolonged elevation of NEFAs and glycerol in serum, as both are used for synthesis of TAG in the liver. Furthermore, under hyperglycemic conditions, an increased glucose flux into the liver in FRic$^{-/-}$ mice could compensate for skeletal muscle insulin resistance to maintain normoglycemia (43). The surplus glucose is converted to TAG and contributes to the development of hepatic steatosis. Thus, liver function also becomes affected in FRic$^{-/-}$ animals after chronic exposure to elevated circulating NEFAs, glycerol, and glucose.

A different line of fat cell–specific rictor knockout mice (referred to as rictor$^{ad-/-}$) has recently been described (21). Rictor$^{ad-/-}$ mice showed that visceral organs such as liver, pancreas, kidney, fat pads, spleen, and heart increased in size with concomitantly increased lean mass that was more apparent on a high-fat diet. This finding suggests that rictor/mTORC2 in fat cells is important for organismal growth (21). Our FRic$^{-/-}$ mice also showed

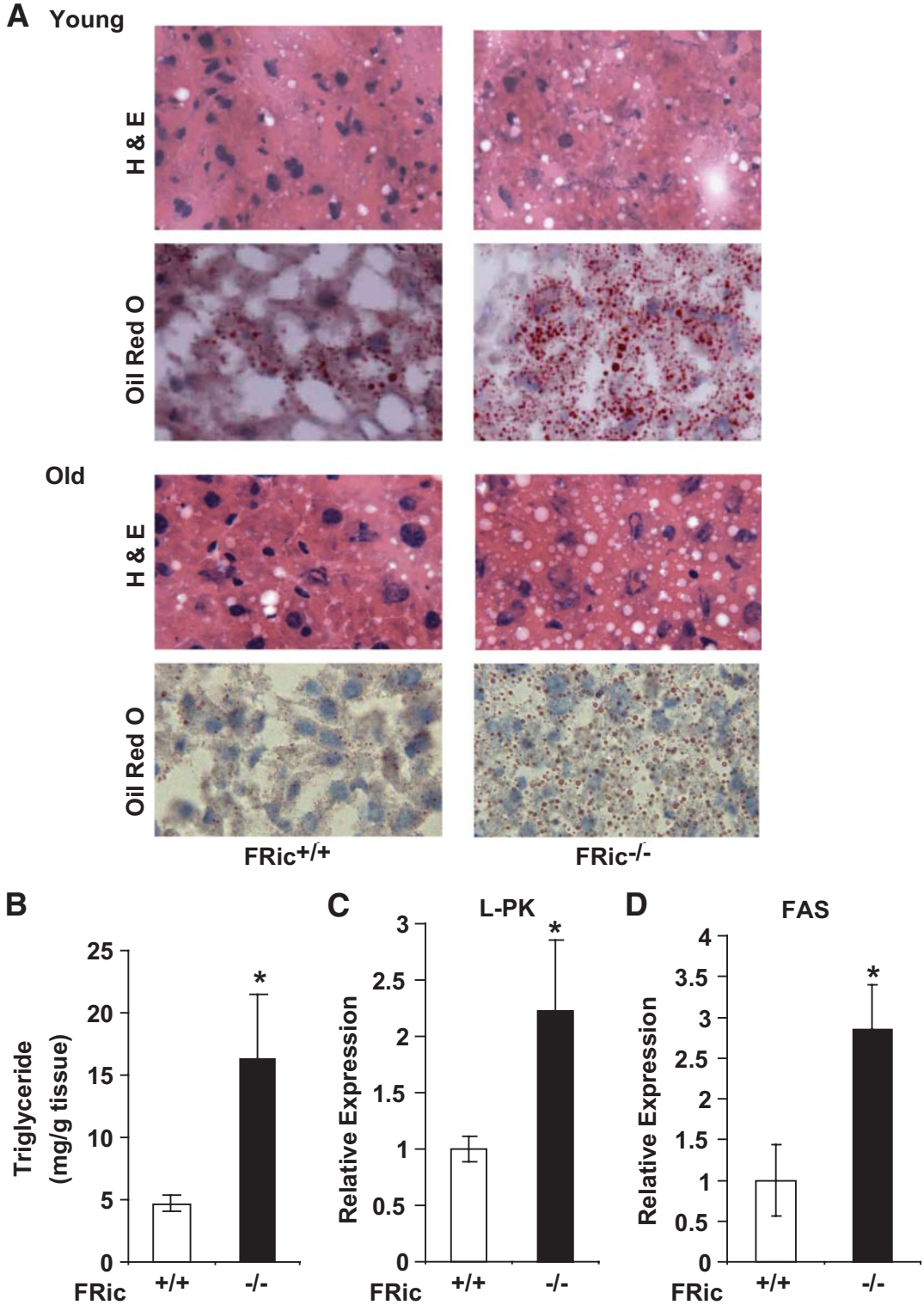

FIG. 6. Hepatic steatosis in FRic$^{-/-}$ mice. *A*: Histochemical analysis of FRic$^{-/-}$ and FRic$^{+/+}$ liver for hepatic steatosis. *A*: Young (2–5 months old) and old (>9 months old) female FRic$^{+/+}$ or FRic$^{-/-}$ mice liver sections stained with hematoxylin and eosin (H & E) (*upper panels*), or oil red O (*lower panels*) (representative images are shown out of four to five for each age-group). *B*: Triglyceride concentration in liver homogenates of FRic$^{+/+}$ and FRic$^{-/-}$ mice (>6-month-old female, $n = 8–9$, *$P < 0.01$). *C* and *D*: Lipogenic gene expression in liver normalized to GAPDH. *C*: L-type pyruvate kinase gene expression (>6-month-old male mice, $n = 5$, *$P < 0.03$). *D*: FAS gene expression (>6-month-old male mice, $n = 5$, *$P < 0.02$). Data shown are means ± SE. (A high-quality digital representation of this figure is available in the online issue.)

increased organ size (supplemental Fig. 3). The rictor$^{ad-/-}$ mice were hyperinsulinemic but were normoglycemic in the fed and fasting state, similar to young FRic$^{-/-}$ mice. Increased pancreatic β-cell mass could contribute to hyperinsulinemia in FRic$^{-/-}$ mice, as suggested for the rictor$^{ad-/-}$ mice. However, increased β-cell mass alone is not sufficient to induce hyperinsulinemia (44) but requires a factor that would induce insulin secretion. It is well known that insulin resistance is compensated by increased β-cell mass and insulin secretion (45). Our results from

hyperinsulinemic-euglycemic clamp studies in FRic$^{-/-}$ mice show severe whole-body insulin resistance including adipose tissue, skeletal muscle, and liver. While the insulin sensitivity in rictor$^{ad-/-}$ mice was not directly measured, results from insulin tolerance tests suggest that these mice are also insulin resistant. Cybulski et al. (21) ascribe the insulin resistance in the rictor$^{ad-/-}$mice to decreased circulating adiponectin levels. There was no change in adiponectin levels in the FRic$^{-/-}$ animals on a standard diet. The reason for this discrepancy is not clear, as both fat cell–specific rictor knockout models have very similar genetic backgrounds of 129 crossed to C57BL/6J, although the 129 substrains differ (129S6 for FRic$^{-/-}$ mice and 129S1/Svlmj for rictor$^{ad-/-}$ mice). However, since the genetic loss of adiponectin does not affect insulin sensitivity of standard diet–fed mice (46), it is unlikely that decreased adiponectin is the cause for decreased insulin sensitivity arising from fat cell–specific loss of rictor in mice. The elevated circulating NEFA levels that we observe in the FRic$^{-/-}$ mice could not only contribute to peripheral insulin resistance but also directly stimulate insulin secretion from β-cells (data not shown) as well as increase pancreatic β-cell mass (47). Therefore, we propose that hyperinsulinemia and increased β-cell mass in FRic$^{-/-}$ mice is predominantly a consequence of insulin resistance and increased NEFAs.

In conclusion, we demonstrate that mTORC2 is essential for insulin action on glucose transport and lipolysis in fat cells. Our studies further demonstrate the important role for mTORC2 in the regulation of fat cell function and control of whole-body glucose and lipid homeostasis and insulin sensitivity. Thus, mTORC2 may serve as a drug target for the treatment of obesity and type 2 diabetes.

ACKNOWLEDGMENTS

This work was supported by National Institutes of Health Grants DK52753 and DK28312 (to J.C.L.) and DK80756 (to J.K.K.), the American Diabetes Association (1-04-RA-47 and 7-07-RA-80 to J.K.K.), and University of Massachusetts Diabetes Endocrinology Research Center Grant DK32520 (to J.K.K.).

No potential conflicts of interest relevant to this article were reported.

Parts of this study were presented at the 68th Scientific Sessions of the American Diabetes Association, San Francisco, CA, 6–10 June 2008.

We thank Drs. James Garrison, Thomas Sturgill (University of Virginia), and Sue Bodine (University of California, Davis) for helpful comments on the manuscript; Dr. Peter Gillespie (Oregon Health and Science University) for providing the Myo1c antibody; and Olesya Shcheglovitova for assistance with mouse husbandry and genotyping.

REFERENCES

1. Wullschleger S, Loewith R, Hall MN. TOR signaling in growth and metabolism. Cell 2006;124:471–484
2. Jacinto E, Loewith R, Schmidt A, Lin S, Ruegg MA, Hall A, Hall MN. Mammalian TOR complex 2 controls the actin cytoskeleton and is rapamycin insensitive. Nat Cell Biol 2004;6:1122–1128
3. Vander HE, Lee SI, Bandhakavi S, Griffin TJ, Kim DH. Insulin signalling to mTOR mediated by the Akt/PKB substrate PRAS40. Nat Cell Biol 2007;9:316–323
4. Sarbassov DD, Ali SM, Sengupta S, Sheen JH, Hsu PP, Bagley AF, Markhard AL, Sabatini DM. Prolonged rapamycin treatment inhibits mTORC2 assembly and Akt/PKB. Mol Cell 2006;22:159–168
5. Hay N, Sonenberg N. Upstream and downstream of mTOR. Genes Dev 2004;18:1926–1945
6. Sarbassov DD, Guertin DA, Ali SM, Sabatini DM. Phosphorylation and regulation of Akt/PKB by the rictor-mTOR complex. Science 2005;307:1098–1101
7. Whiteman EL, Cho H, Birnbaum MJ. Role of Akt/protein kinase B in metabolism. Trends Endocrinol Metab 2002;13:444–451
8. Alessi DR, Andjelkovic M, Caudwell B, Cron P, Morrice N, Cohen P, Hemmings BA. Mechanism of activation of protein kinase B by insulin and IGF-1. EMBO J 1996;15:6541–6551
9. Guertin DA, Stevens DM, Thoreen CC, Burds AA, Kalaany NY, Moffat J, Brown M, Fitzgerald KJ, Sabatini DM. Ablation in mice of the mTORC components raptor, rictor, or mLST8 reveals that mTORC2 is required for signaling to Akt-FOXO and PKCalpha, but not S6K1. Dev Cell 2006;11:859–871
10. Shiota C, Woo JT, Lindner J, Shelton KD, Magnuson MA. Multiallelic disruption of the rictor gene in mice reveals that mTOR complex 2 is essential for fetal growth and viability. Dev Cell 2006;11:583–589
11. Kumar A, Harris TE, Keller SR, Choi KM, Magnuson MA, Lawrence JC, Jr. Muscle-specific deletion of rictor impairs insulin-stimulated glucose transport and enhances Basal glycogen synthase activity. Mol Cell Biol 2008;2008;28:61–70
12. Kershaw EE, Flier JS. Adipose tissue as an endocrine organ. J Clin Endocrinol Metab 2004;89:2548–2556
13. Ruan H, Lodish HF. Regulation of insulin sensitivity by adipose tissue-derived hormones and inflammatory cytokines. Curr Opin Lipidol 2004;15:297–302
14. Morrisett JD, Abdel-Fattah G, Hoogeveen R, Mitchell E, Ballantyne CM, Pownall HJ, Opekun AR, Jaffe JS, Oppermann S, Kahan BD. Effects of sirolimus on plasma lipids, lipoprotein levels, and fatty acid metabolism in renal transplant patients. J Lipid Res 2002;43:1170–1180
15. Morrisett JD, Abdel-Fattah G, Kahan BD. Sirolimus changes lipid concentrations and lipoprotein metabolism in kidney transplant recipients. Transplant Proc 2003;35:143S–150S
16. Abel ED, Peroni O, Kim JK, Kim YB, Boss O, Hadro E, Minnemann T, Shulman GI, Kahn BB. Adipose-selective targeting of the GLUT4 gene impairs insulin action in muscle and liver. Nature 2001;409:729–733
17. Kim HJ, Higashimori T, Park SY, Choi H, Dong J, Kim YJ, Noh HL, Cho YR, Cline G, Kim YB, Kim JK. Differential effects of interleukin-6 and -10 on skeletal muscle and liver insulin action in vivo. Diabetes 2004;53:1060–1067
18. Garcia-Martinez JM, Alessi DR. mTOR complex 2 (mTORC2) controls hydrophobic motif phosphorylation and activation of serum- and glucocorticoid-induced protein kinase 1 (SGK1). Biochem J 2008;416:375–385
19. Facchinetti V, Ouyang W, Wei H, Soto N, Lazorchak A, Gould C, Lowry C, Newton AC, Mao Y, Miao RQ, Sessa WC, Qin J, Zhang P, Su B, Jacinto E. The mammalian target of rapamycin complex 2 controls folding and stability of Akt and protein kinase C. EMBO J 2008;27:1932–1943
20. Ikenoue T, Inoki K, Yang Q, Zhou X, Guan KL. Essential function of TORC2 in PKC and Akt turn motif phosphorylation, maturation and signalling. EMBO J 2008;27:1919–1931
21. Cybulski N, Polak P, Auwerx J, Ruegg MA, Hall MN. mTOR complex 2 in adipose tissue negatively controls whole-body growth. Proc Natl Acad Sci U S A 2009;106:9902–9907
22. Keller SR. The insulin-regulated aminopeptidase: a companion and regulator of GLUT4. Front Biosci 2003;8:s410–s420
23. Huang S, Czech MP. The GLUT4 glucose transporter. Cell Metab 2007;5:237–252
24. Holm C. Molecular mechanisms regulating hormone-sensitive lipase and lipolysis. Biochem Soc Trans 2003;31:1120–1124
25. Yeaman SJ. Hormone-sensitive lipase: new roles for an old enzyme. Biochem J 2004;379:11–22
26. Smith U. Impaired ('diabetic') insulin signaling and action occur in fat cells long before glucose intolerance–is insulin resistance initiated in the adipose tissue?. Int J Obes Relat Metab Disord 2002;26:897–904
27. Harris TE, Huffman TA, Chi A, Shabanowitz J, Hunt DF, Kumar A, Lawrence JC, Jr. Insulin controls subcellular localization and multisite phosphorylation of the phosphatidic acid phosphatase, lipin 1. J Biol Chem 2007;282:277–286
28. Sano H, Kane S, Sano E, Miinea CP, Asara JM, Lane WS, Garner CW, Lienhard GE. Insulin-stimulated phosphorylation of a Rab GTPase-activating protein regulates GLUT4 translocation. J Biol Chem 2003;278:14599–14602
29. Sano H, Eguez L, Teruel MN, Fukuda M, Chuang TD, Chavez JA, Lienhard GE, McGraw TE. Rab10, a target of the AS160 Rab GAP, is required for insulin-stimulated translocation of GLUT4 to the adipocyte plasma membrane. Cell Metab 2007;5:293–303
30. Kitamura T, Kitamura Y, Kuroda S, Hino Y, Ando M, Kotani K, Konishi H, Matsuzaki H, Kikkawa U, Ogawa W, Kasuga M. Insulin-induced phosphor-

ylation and activation of cyclic nucleotide phosphodiesterase 3B by the serine-threonine kinase Akt. Mol Cell Biol 1999;19:6286–6296
31. Duncan RE, Ahmadian M, Jaworski K, Sarkadi-Nagy E, Sul HS. Regulation of lipolysis in adipocytes. Annu Rev Nutr 2007;27:79–101
32. Choi YH, Park S, Hockman S, Zmuda-Trzebiatowska E, Svennelid F, Haluzik M, Gavrilova O, Ahmad F, Pepin L, Napolitano M, Taira M, Sundler F, Stenson HL, Degerman E, Manganiello VC. Alterations in regulation of energy homeostasis in cyclic nucleotide phosphodiesterase 3B-null mice. J Clin Invest 2006;116:3240–3251
33. Polak P, Cybulski N, Feige JN, Auwerx J, Ruegg MA, Hall MN. Adipose-specific knockout of raptor results in lean mice with enhanced mitochondrial respiration. Cell Metab 2008;8:399–410
34. Defronzo RA. Pathogenesis of type 2 (non-insulin dependent) diabetes mellitus: a balanced overview. Diabetologia 1992;35:389–397
35. Kim JK, Gimeno RE, Higashimori T, Kim HJ, Choi H, Punreddy S, Mozell RL, Tan G, Stricker-Krongrad A, Hirsch DJ, Fillmore JJ, Liu ZX, Dong J, Cline G, Stahl A, Lodish HF, Shulman GI. Inactivation of fatty acid transport protein 1 prevents fat-induced insulin resistance in skeletal muscle. J Clin Invest 2004;113:756–763
36. Petersen KF, Shulman GI. Etiology of insulin resistance. Am J Med 2006;119:S10–S16
37. Yuan M, Konstantopoulos N, Lee J, Hansen L, Li ZW, Karin M, Shoelson SE. Reversal of obesity- and diet-induced insulin resistance with salicylates or targeted disruption of Ikkbeta. Science 2001;293:1673–1677
38. Hirosumi J, Tuncman G, Chang L, Gorgun CZ, Uysal KT, Maeda K, Karin M, Hotamisligil GS. A central role for JNK in obesity and insulin resistance. Nature 2002;420:333–336
39. Griffin ME, Marcucci MJ, Cline GW, Bell K, Barucci N, Lee D, Goodyear LJ, Kraegen EW, White MF, Shulman GI. Free fatty acid-induced insulin resistance is associated with activation of protein kinase C theta and alterations in the insulin signaling cascade. Diabetes 1999;48:1270–1274
40. Shulman GI. Cellular mechanisms of insulin resistance. J Clin Invest 2000;106:171–176
41. Zhang J, Gao Z, Yin J, Quon MJ, Ye J. S6K Directly Phosphorylates IRS-1 on Ser-270 to Promote Insulin Resistance in Response to TNF-{alpha} Signaling through IKK2. J Biol Chem 2008;283:35375–35382
42. Werner ED, Lee J, Hansen L, Yuan M, Shoelson SE. Insulin resistance due to phosphorylation of insulin receptor substrate-1 at serine 302. J Biol Chem 2004;279:35298–35305
43. Bruning JC, Michael MD, Winnay JN, Hayashi T, Horsch D, Accili D, Goodyear LJ, Kahn CR. A muscle-specific insulin receptor knockout exhibits features of the metabolic syndrome of NIDDM without altering glucose tolerance. Mol Cell 1998;2:559–569
44. Rosen ED, Kulkarni RN, Sarraf P, Ozcan U, Okada T, Hsu CH, Eisenman D, Magnuson MA, Gonzalez FJ, Kahn CR, Spiegelman BM. Targeted elimination of peroxisome proliferator-activated receptor gamma in beta cells leads to abnormalities in islet mass without compromising glucose homeostasis. Mol Cell Biol 2003;23:7222–7229
45. Bruning JC, Winnay J, Bonner-Weir S, Taylor SI, Accili D, Kahn CR. Development of a novel polygenic model of NIDDM in mice heterozygous for IR and IRS-1 null alleles. Cell 1997;88:561–572
46. Maeda N, Shimomura I, Kishida K, Nishizawa H, Matsuda M, Nagaretani H, Furuyama N, Kondo H, Takahashi M, Arita Y, Komuro R, Ouchi N, Kihara S, Tochino Y, Okutomi K, Horie M, Takeda S, Aoyama T, Funahashi T, Matsuzawa Y. Diet-induced insulin resistance in mice lacking adiponectin/ACRP30. Nat Med 2002;8:731–737
47. Lingohr MK, Buettner R, Rhodes CJ. Pancreatic beta-cell growth and survival: a role in obesity-linked type 2 diabetes?. Trends Mol Med 2002;8:375–384